

THE ENERGY DISTRIBUTION MECHANISMS OF THE NEAR WAKES OF PLANETARY ENTRY PROBES

Sudantha Balage⁽¹⁾, Russell Boyce⁽²⁾, Neil Mudford⁽¹⁾, Sean O'Byrne⁽¹⁾

⁽¹⁾UNSW@ADFA, School of ACME, Canberra, Australia Email: s.balage@adfa.edu.au

⁽²⁾University of Queensland, Division of Mechanical Engineering, Brisbane, Australia Email: Russell.boyce@uq.edu.au

ABSTRACT

A CFD aided theoretical analysis is reported of the energy exchange and conversion processes occurring in the near wakes of bluff bodies in hypersonic flight. The study proceeds by first selecting a point on the Mars atmospheric entry trajectory of the Beagle II spacecraft as the datum case. The freestream values of the system π groups are then varied in a systematic fashion and the flowfield is recalculated in order to discover the underlying dependence on π groups of the two phenomena of particular interest. The first of these is the presence an aft facing shock in the reverse flow ahead of the aft stagnation point on the body. The second is a newly identified phenomenon of wake flow thermal inversion in which total temperatures in the near wake flow are elevated above those of the freestream by strong viscous coupling of the external flow driving the wake vortex coupled with poor heat transfer out of the wake. Cyclic heating and cooling behavior is examined for closed streamlines in the wake as further evidence of the energy exchange origins of the thermal inversion observed in the computed flows.

1. INTRODUCTION

The forebody heat transfer of capsules has been studied since the dawn of the space age. Information on the afterbody heat transfer and the wake flow aerothermodynamics, however, remains sparse. In both Earth and Mars re-entry, paintwork at the base of a capsule has been reported to have survived the entry process indicating very low afterbody temperatures. Both flight and ground tests have, however, measured base temperatures that are higher than the predictions made by computational fluid dynamics. Various models that compute transport quantities for the CFD computations disagree, particularly at high temperatures. This situation leaves both theoretical and experimental uncertainty associated with hypersonic wake flows. The large uncertainty in the base temperatures of re-entry capsule has motivated this CFD based theoretical exploration of the wakes of re-entry craft at hypersonic velocities.

In this study, a technique based on non-dimensional quantities is deployed in conjunction with CFD computations. The basic approach is to first identify the

π groups associated with the phenomena of interest and then, by considering the associated terms of the Navier-Stokes equations, propose a 'sub equations' that represents the physics of the phenomena. While the study concentrates on hypersonic bluff body wakes, the techniques developed and some findings are general enough to apply to driven vortex flow such as those found in hypersonic flow over steps, cavities and wedges.

2. WAKE ENERGY RECOVERY

Computational fluid dynamics is initially used to compute a datum flowfield. The input flow parameters are then changed so that one π groups at a time is modified to identify the flow dynamics in a general yet simple manner. The steady state simulations of axisymmetric capsule geometry of Beagle II Mars entry craft [2] are performed using calorically perfect CO₂ gas and adiabatic wall boundaries. Under these assumptions, any flow quantity Q , can be represented by $Q = Q(\text{Re}, M, \gamma, \text{Pr})$, a four-similarity parameter (π group) function where the symbols have their usual meanings. The ratio of specific heats, γ , is kept constant at $\gamma = 1.333$.

Two main phenomena of interest for this investigation are the recovered wall temperature, T_{base} , at the center of the capsule base and the presence or absence of the so-called wake reverse flow shock (WRFS) that has been observed in some previous computational studies. Accordingly, the Q quantities are chosen as $Q_1 = T_{\text{base}}/T_{\text{tot}}$ and $Q_2 = M_{\text{b_max}}$ where T_{tot} is the freestream total temperature and $M_{\text{b_max}}$ is the maximum reverse flow Mach number in the wake. Q_1 and Q_2 form the axes of the wake energy recovery plot (WERP) shown for the present flows in Fig. 1.

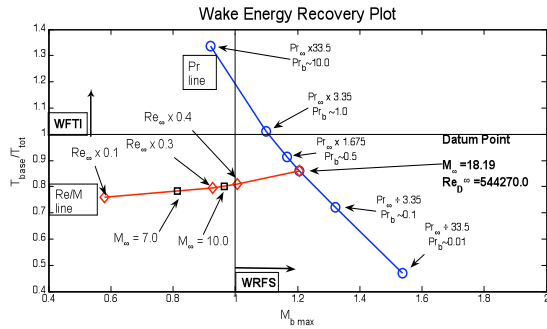


Figure 1. The WERP indicating the regions with wake reverse flow shock (WRFS) and the wake flow thermal inversion (WFTI) in CFD solutions.

The flow field is initially simulated at a datum re-entry condition of 4000m/s velocity, 54Pa static pressure and 193K static temperature in the oncoming flow [1]. Further values of Q_1 and Q_2 are obtained by changing boundary conditions such that the similarity parameters computed with far field conditions, Re_{∞} , M_{∞} and Pr_{∞} , are changed independently from each other from the datum values. The more vertical line on Fig. 1, referred to here as the Prandtl line, shows the effect of the Prandtl number while the nearly horizontal line shows that of both freestream Reynolds and Mach numbers. Reynolds and Mach data are observed to vary Q_1 and Q_2 so as to trace out a single line on the WERP within the range and the uncertainty of the present study. We shall call this line Reynolds/Mach line. The calculations reveal that the reverse flow Mach number is strongly dependent on free stream Reynolds and Mach numbers. At sufficiently high free stream Reynolds and Mach numbers, the reverse flow becomes supersonic[3], leading to a wake reverse flow shock (WRFS).

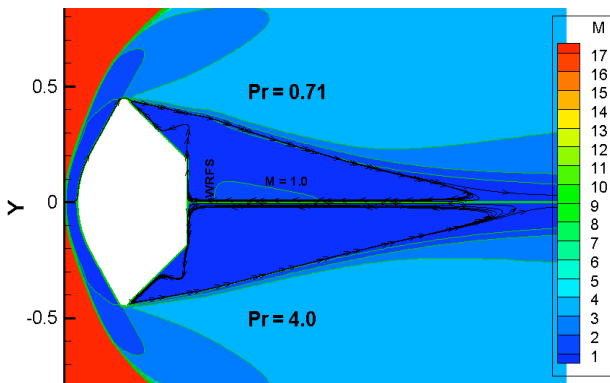


Figure 2. The $Pr = 4.0$ solution has the WRFS suppressed due to the high wake temperature resulting from high Prandtl number.

The WERP indicates the important role of the wake region Prandtl number as the ‘governor’ of the wake region temperature. The base temperature ratio

(T_{base}/T_{tot}) is observed to be only weakly, if at all, dependent on freestream Reynolds and Mach numbers. The recovered base temperature ratio is however strongly dependent on the wake Prandtl number consequently, the uncertainty associated with the base temperature ratio is also related to that of the wake Prandtl number. Therefore, in CFD computations for example, the modeling uncertainties associated with the computation of viscosity μ , thermal conductivity k and heat capacity c_p have an effect on the computed recovered base temperature ratio and wake region temperatures in general.

The analysis of the CFD solutions show that the influence of the Prandtl number in the wake vortex is predominantly in its thermal component and not in its specific kinetic energy, $u^2/2$. This is also evident in the negative gradient of the Prandtl curve observed in Fig. 1. Therefore the reverse flow shock can be quenched by high wake Prandtl numbers (See Fig. 2) and enhanced by low wake Prandtl numbers.

The simulations also predict that the wake flow would reach a higher total temperature than the free stream flow at wake Prandtl number of unity. This phenomenon is termed the wake flow thermal inversion (WFTI)[1] and remains a theoretical possibility, though it believed to be not been observed in hypersonic bluff body wakes. The effect of Pr on the wake flow total temperature is shown in Fig. 3 below. For flows with $Pr < 1$, the wake center has the minimum total temperature. For $Pr > 1$ however, the wake flow has the ‘inverted’ total temperature distribution where the wake center has the maximum total temperature. Note that other features of the flows, such as the wake flow boundaries are not dramatically dissimilar for the two cases. This derives from the fact that $Re_{D,\infty}$ and M_{∞} are the same for both flows depicted and for the datum flow.

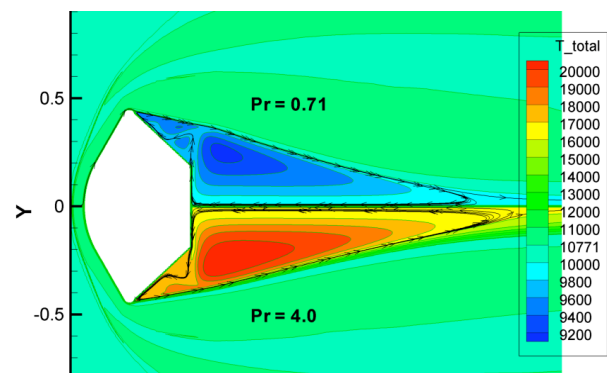


Figure 3. WFTI is evident on $Pr = 4.0$ solutions total temperature field. The total temperature far outside the dividing streamline (outside the wake ‘boundary layer’) is not influenced by the Prandtl number effects.

3. BASE PRESSURE RECOVERY

Prandtl number variation also has a strong influence on wake flow total pressures. The base stagnation pressure p_b , normalized with the nose stagnation pressure, p_n , can be chosen as a third parameter of interest, $Q_3 = P_b/P_n$, to generate a wake pressure recovery plot (WPRP). The ratio of the nose to base pressure, P_b/P_n , in the hypersonic limit, for many experiments, is reported to be in the vicinity of 2 - 4.% in the literature [4]. This is confirmed in all CFD simulations of the present study as well. Fig. 4 indicates that the Prandtl number, and the free stream Mach and Reynolds numbers significantly influence the recovered base pressure. Therefore, a part of the uncertainty in computing the base pressure stems from that of the computation of the wake Prandtl number. The wake Prandtl number, through its influence on the recovered base pressure, has an influence in the total drag force experienced by the capsule though its overall contribution may not be significant in the hypersonic limit.

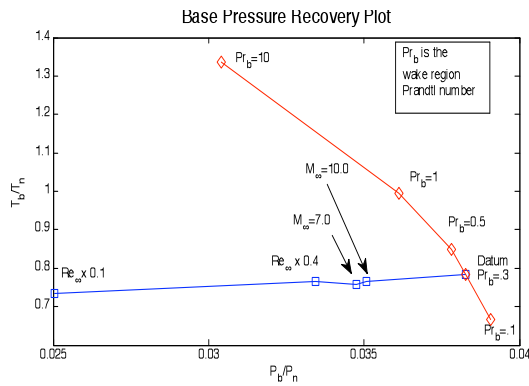


Figure 4. The recovered pressure at the base normalized with capsule nose pressure is plotted with recovered temperature ratio of the same locations.

The axes of the base pressure recovery plot (BPRP) above are the terms required to compute the entropy increase between the nose and the base via the Gibbs equation. Therefore it can be seen that BPRP also indicates the role of the Prandtl number in determining the entropy in the wake region.

4. IDEAL DRIVEN VORTEX

In order to explain the above observations we shall first construct an ideal example of a driven vortex illustrated in Fig. 5. This ideal vortex is two-dimensional and is driven by an external flow whose nature prevents the vortex flow from becoming a rigid body motion.

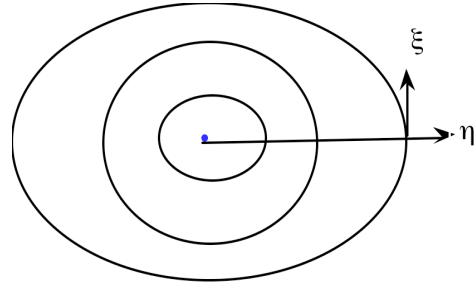


Figure 5. The ideal driven vortex with general, orthogonal, co-ordinate η and the tangential co-ordinate ζ . The surfaces defined by the streamlines are perpendicular to the page.

The external driving flow and the vortex flow are separated by a dividing streamline, which is closed. The vortex flow consists of closed streamlines with a constant speed along each streamline. The outside flow is made to have a single total enthalpy and Mach number to simplify our analysis.

While there is no mass flow across the streamlines, heat and work are exchanged across them. The normal velocity profile of the vortex is monotonic with zero velocity at the center giving the direction of the viscous work done to be from outside to interior. A part of the work done is converted into heat, via the viscous interactions, and the rest of the work is transferred deeper into the vortex interior. At steady state conditions, the work done on a given streamline by the flow external to it should equal the heat transferred across the streamline to that external flow. From the thermal point of view the vortex is an enclosed region with a volumetric heat production source term and, regardless of the normal distribution of any positive source term, the maximum temperature then lies always at the interior when the steady state is reached. The heat flux therefore is always directed from interior to exterior. We can express the above defined steady state vortex physics via Equation (1) below.

$$\frac{\dot{W}}{\dot{q}} = \frac{\oint \mu u \frac{\partial u}{\partial \eta} dS_L}{\oint -k \frac{\partial T}{\partial \eta} dS_L} = 1 \quad (1)$$

Where S_L is the surface area of the closed streamline at $\eta = L$ in the driven vortex, \dot{W} is viscous rate of work done by the driving flow across S_L , \dot{q} is the rate of heat emitted by the vortex across S_L , μ viscosity and k thermal conductivity.

Re arranging the above equation (1) we have,

$$\oint \left[\text{Pr} \frac{\partial \left(\frac{u^2}{2} \right)}{\partial \eta} - \frac{\partial (c_p T)}{\partial \eta} \right] dS_L = 0 \quad (2)$$

Note that the equations (1) and (2) are global statements about the conservation of energy, or the work-energy theorem of the steady state vortex flow. The validity of this expression is based on the assumption that the derivatives exist and are non-zero, that it is the vortex is not executing rigid body motion. Equation (2) excludes the effects other than viscous and thermal diffusion of the momentum energy transport such as pressure and bulk work done or radiative heat transfer. No symmetry of the flow is assumed.

If the flow conditions are axisymmetric, a local expression of the above equation (2) can be made to hold generally. That is, for symmetric vortices, the integrand of equation (2) should be zero, implying

$$\text{Pr} d \left(\frac{u^2}{2} \right) + d(c_p T) = 0 \quad (3)$$

where the differentials are in the normal direction. Note however, that the symmetry of the vortex is not a necessary condition for flow to satisfy equation (3).

The differential equation (3) has a linear solution and the solution can be represented in an enthalpy-kinetic energy, or a H-K diagram, as shown in Fig. 6.

The equation (3) acts as a ‘constraint’ on the H-K data of the driven vortex. The solution line starts from the

point determined by the total enthalpy and the Mach number (h_0, M) of the dividing streamline and moves with a gradient whose value is the negative of the Prandtl number. At the vortex centre, the flow has the maximum temperature and zero velocity. In the inverted solution ($\text{Pr} > 1$) the vortex center has the maximum total enthalpy and in the un-inverted ($\text{Pr} < 1$) case vortex has the minimum total enthalpy at the center.

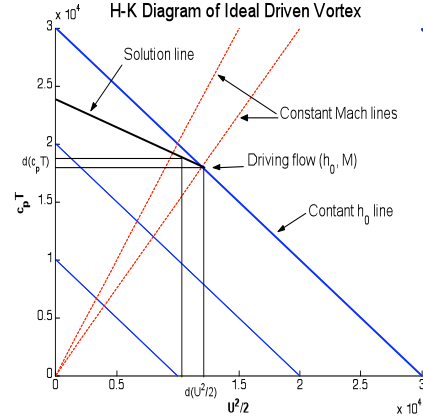


Figure 6. The solution of the equation (3) for the Prandtl number less than unity.

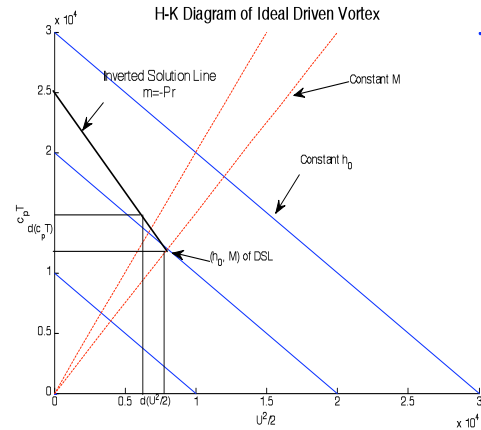


Figure 7. When $\text{Pr} > 1$, the conservation of energy, represented by eqn. (3), predicts thermal inversion.

5. NEAR WAKE VORTICES

The steady state near wakes of a bluff body consists of a vortex with closed streamlines driven by a free shear layer originating in the shock layer on the forebody. The vortex flow, due to its close looped streamlines, is trapped in the near wake and the driving flow external to it only makes a single pass through the near wake region. The streamline that separates the above two distinct flow regions is called the dividing streamline and goes through a four-way bifurcation at the rear stagnation point. Work and heat are exchanged

between the two flow regions, and at equilibrium the rate of work done across the dividing streamline balances the rate of heat transfer across it provided the rear wall of the bluff body is adiabatic.

There are differences between the near wake vortices in the base flow and the ideal driven vortex studied in the previous section. One notable difference is the existence of the stagnation regions in the near wake vortices. The so called $u = 0$ line, where the horizontal component of the flow velocity is zero due to the turning of the flow, signifies a type of stagnation where the balance of the shear and pressure forces cause the flow to slow down and to turn around without any external device or influence such as a presence of a wall or a bulk external force. Note also that in the near wake vortex the Mach number along the dividing streamline is not a constant due to the flow stagnations and accelerations.

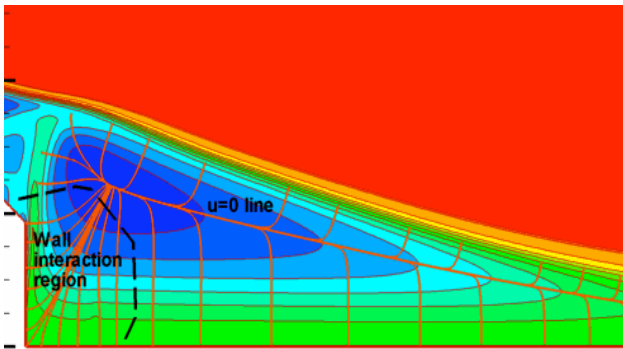


Figure 8. The η (general normal) co-ordinate directions are marked by the brown lines against the total temperature contour lines for the datum condition flow solution. The approximate region where the wall has an influence over the vortex flow is marked. In the background contour lines, blue represents low total temperature and red represents high total temperature.

When a wall is present in the vortex flow, as in for the base region of a re-entry capsule, it also changes the boundary conditions of the driven vortex from that of the ideal case. The presence of a wall causes the streamlines not only to stagnate with a corresponding pressure and temperature increase but also to have extended zero velocity lines due to the wall boundary conditions. This changes the velocity profile of the vortex from being a monotonically increasing function from its center value of zero to the maximum at the outermost streamline, as was supposed for the ideal vortex, to a flow that has the maximum speed between the center and the wall. In such circumstances, the direction of the shear work done is no longer uniquely pointed towards the center of the vortex. The shear work reverses direction after the position of the maximum flow speed along a normal co-ordinate that links the

wall to the vortex center. Similarly, the stagnation of the streamlines interacting with the wall would cause the heat fluxes to have a component pointing towards the center of the vortex. Therefore, the wall, within its domain of influence, can locally change the direction of the work and heat transfer inside a driven vortex.

Let us choose the (η, ξ) co-ordinate system to investigate the wake vortex. The system is orthogonal at each point of the wake however, due to the flow speedup and slowdown the co-ordinate directions are deformed in the wake vortex compared to that of the ideal vortex. Fig. 8 shows the η co-ordinate directions ($\xi = \text{constant}$ lines) of the main wake vortex of the Beagle II at the datum flow conditions. These $\xi = \text{constant}$ lines shows two distinct regions of asymptotic behavior, the horizontal one, to the $u = 0$ line and the more vertical one, due to the base stagnation. The H-K data extracted along the $\xi = \text{constant}$ lines (see Fig. 9) which are asymptotic to $u = 0$ line falls close to the Prandtl line (gradient, $m = -0.338 = -(\text{wake Pr})$) of the corresponding driving flow Mach number (see fig. 10). This means that, in this region, the local form of the viscous/thermal interactions, i.e., the equation (3) holds true, to a close approximation, and has similar physics to the ideal symmetric vortex. That is, the work is done by the external flow to the interior flow and the heat is transferred from interior to the external flow with a linear relationship which has the Prandtl number as the gradient of H-K relationship. The H-K data extracted along $\xi = \text{constant}$ lines which starts at the wall and the stagnation region due to the base, do not have a linear H-K relationship as expected from our reasoning (see fig. 11).

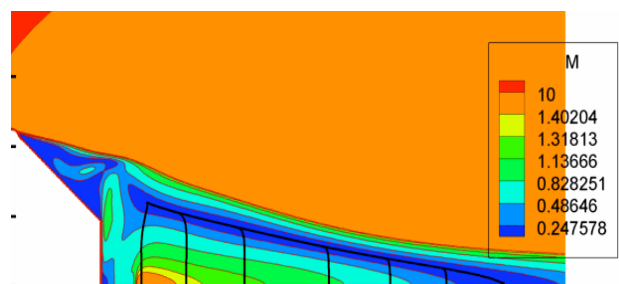


Figure 9. The H-K data in Fig. 10 are extracted along the $\xi = \text{const}$ lines shown above. The background contours are that of the Mach number.

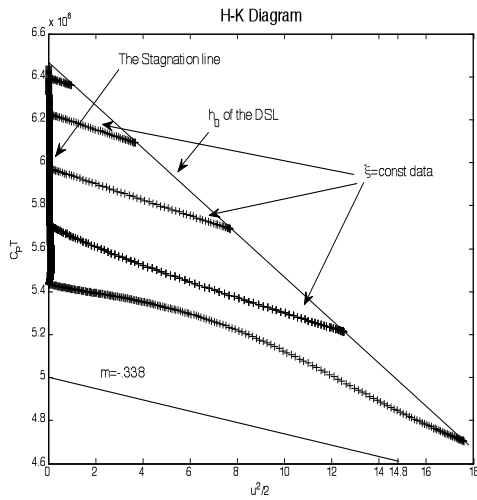


Figure 10. The specific enthalpy-specific kinetic energy (H-K) data extracted along the $\xi = \text{const}$ lines of Fig. 9.. The bottom line, taken from the location of the maximum reverse flow Mach number shows the influence of the stagnation due to the wall in the mid section.

The deviations from the linear relationship of the H-K data along the $\xi = \text{constant}$ lines can, at least in part, be attributed to the influence of the wall interaction regions. The H-K data obtained closer to the wall interaction region show bigger deviations from the linear relationship.

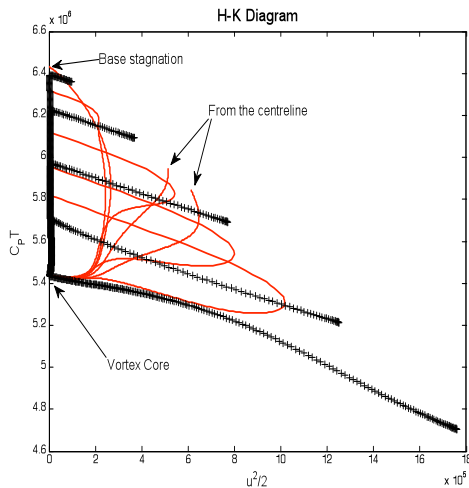


Figure 11. The continuous red lines show the H-K data taken along the $\xi = \text{const}$ lines that lie within the domain of influence of the wall.

The consequences of the shifting of the energy due to the interaction of the wall can be investigated by observing the temperature-entropy (T-S) data of a closed streamline. Fig. 12 shows a closed wake

streamline of the datum flow solution and the T-S diagram of the fluid element that follows the streamline is plotted on the fig. 13.

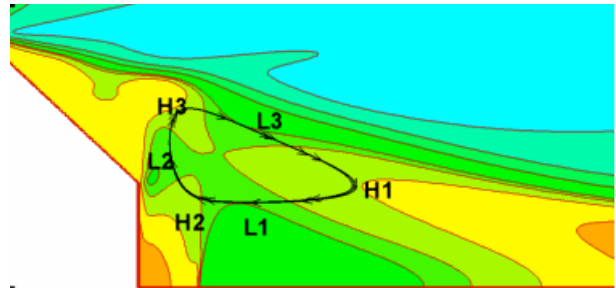


Figure 12. The closed streamlines where entropy and temperature data are extracted. The background contour lines are that of the temperature.

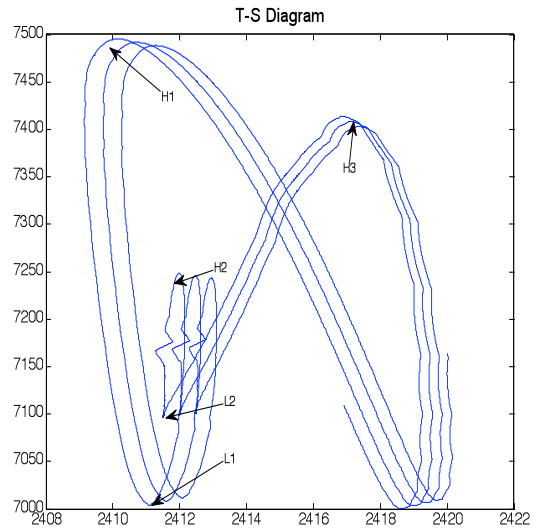


Figure 13. The T-S data for the closed streamline in Fig. 12 indicating the heating and cooling cycles due to accelerations and stagnations of the flow.

The above fig. 13 indicates the existence of heating and cooling cycles as a fluid element traverses along the streamline.

6. DISCUSSION AND CONCLUSIONS

The WERP contains information that can aid in the experimental search for wake reverse flow shocks. By uncollapsing the Reynolds/Mach curve, for the flow parameters (h_0 , M) of a given test facility, one could obtain the body length scales of the model that would have a WRFS in its CFD predictions.

This study reveals how the uncertainties associated with transport quantities and c_p can influence the CFD predictions of the base region temperatures and pressure for steady state bluff body wakes. Present work hints at the possible existence of a reactions based enhancement of the effective thermal conductivity to account for very low base temperatures that are experimentally observed.

The analysis conducted for several wake Prandtl numbers show that the role of the Prandtl number on the wake is in determining the ratio of kinetic to thermal component of the flow.

As a fluid element travels along a closed streamlines of a wake vortex it goes through heating and cooling cycles due to flow stagnations and accelerations.

7. REFERENCES

1. Balage, S., Boyce, R., Mudford, N., Ranadive, H., Gai, S. (2007) Similarity Laws of Re-Entry Aerodynamics- Analysis of Reverse Flow Shock and Wake Flow Thermal Inversion Phenomena. International Symposium on Shock Waves (ISSW-26), Gottingen, Germany.
2. Liever, P. A., Habchi, S. D., Burnell S. J., Lingrad, J.S. (2003). Computational Fluid Dynamics Prediction of Beagle 2 Aerodynamic Database. Journal of Spacecraft and Rockets, 40, No5. 632-638.
3. Gnoffo, P.A. Planetary-Entry Gas Dynamics. (1999). Annu. Rev. Fluid Mech. 31, 459-494.
4. Park, G. Gai, S. L., Neely, A. J., Hruschka, R. (2007). Base Pressure and Heat Transfer on Planetary Entry Type Configurations. International Symposium on Shock Waves (ISSW-26), Gottingen, Germany.